



Long-Term Evolution of the Caspian Sea Thermohaline Properties Reconstructed in an Eddy-Resolving OGCM

Gleb S. Dyakonov^{1,2} and Rashit A. Ibrayev^{1,2,3}

¹Northern Water Problems Institute, Russian Academy of Sciences, Petrozavodsk, Russia

²Shirshov Institute of Oceanology, Russian Academy of Sciences, Moscow, Russia

³Marchuk Institute of Numerical Mathematics, Russian Academy of Sciences, Moscow, Russia

Correspondence: Gleb Dyakonov (gleb.gosm@gmail.com)

Abstract. The decadal variability of the Caspian Sea thermohaline properties is investigated by means of a high-resolution ocean general circulation model including sea ice thermodynamics and air-sea interaction, forced by prescribed realistic atmospheric conditions and riverine runoff. The model describes synoptic, seasonal and climatic variations of the sea thermohaline structure, water balance and level height. A reconstruction experiment was conducted for the period of 1961-2001, covering a major regime shift in the global climate of 1976-1978, which allows to investigate the Caspian Sea response to such significant episodes of climate change. The long-term trends in the sea circulation patterns are considered with an assessment of the influence of model error accumulation.

Copyright statement.

1 Introduction

The Caspian Sea is the largest enclosed water body on earth, covering over 370 000 km², and has a catchment area, that is almost 10 times greater. Yet it is highly sensitive to variations in the global climate system as well as the regulation of river runoff and other economic activities in the region. This is vividly reflected in the evolution of the Caspian Sea level, which is subject to large fluctuations both on seasonal and decadal timescales. The water balance of the isolated sea varies significantly due to seasonal character of the riverine discharge, which accounts for level oscillations with an amplitude of 20–40 cm. Long-term fluctuations of the level are even larger: in the second half of the 20th century they amounted to 2.5 m.

Prediction of the impact of global climate changes and man-made activities on the Caspian in the long term represents a great scientific challenge and is an important task for fisheries, coastal development and other industries of the region. Ocean general circulation models (OGCM) have greatly advanced our understanding of the Caspian Sea circulation patterns, particularly its seasonal variability (Arpe et al., 1999; Ibrayev, 2008; Kara et al., 2010; Ibrayev et al., 2010; Gunduz and Özsoy, 2014; Diansky et al., 2016). Furthermore, production of global atmospheric reanalysis datasets, covering extended periods of time (usually decades), made possible a retrospective study of the long-term evolution of a marine environment, based on numerical reconstruction of its response to external forcing, which is a subject of the present paper. This approach was applied in our



previous work (Dyakonov and Ibrayev, 2018) with the emphasis on the long-term variability of the Caspian Sea water balance and its sensitivity. Now we use the same model to study the evolution of thermohaline properties (temperature, salinity and density) of the Caspian in 1960-2000. The period is particularly interesting, as it covers one of the most notable events of global climate change – the climate shift of 1976-1978, also referred to as the Great Pacific Climate Shift, widely discussed in literature (Miller et al., 1994; Wooster and Zhang, 2004; Powell and Xu, 2011). The shift was associated with a change of many climatic processes, including the North Atlantic Oscillation, which led to a significant increase of cyclonic activity and air humidity in Europe and, as a consequence, to a sharp rise of the Caspian Sea level and a change of the stratification type of its waters (Tuzhilkin et al., 2011). In turn this weakened deep water ventilation and caused general degradation of the ecological situation in the sea.

Section 2 provides a description of the numerical experiment conducted, including the model design. Section 3 briefly considers the evolution of the atmospheric and riverine forcing, prescribed in the model. In section 4 we discuss the model results and analyze the obtained circulation patterns and their response to climatic variations.

2 Experiment setup

2.1 Model description

In (Ibrayev, 2001; Ibrayev et al., 2001, 2010) a three-dimensional primitive equation numerical model MESH (Model for Enclosed Sea Hydrodynamics) was presented, which was developed to study the Caspian Sea seasonal variability. The model successfully coped with this task and was used as a basis in the present research. However, an investigation of the Caspian Sea circulation on a decadal timescale imposes additional requirements on the model, so it has been considerably redesigned. Geopotential vertical coordinate (z -coordinate), which had been used in MESH, was replaced by a hybrid system with a terrain-following sigma coordinate covering the upper 30 m sea layer including all of the shallow regions, and a z -coordinate below the 30 m depth. The long-term fluctuations of the Caspian Sea surface height (CSSH) are greater than the seasonal by an order of magnitude and can cause numerical instabilities and errors in a z -coordinate model. The use of a sigma coordinate ensures model stability during CSSH lows and allows much better resolution of the surface boundary layer structure and, in turn, the diurnal air-sea interaction cycle during the CSSH highs. A sigma coordinate grid also provides an accurate representation of the Northern Caspian shelf bathymetry with increasingly flat slope (see fig. 1). This is necessary to reconstruct the evolution of the sea surface area and, in turn, the evolution of air-sea fluxes, which are subject to significant variability due to large CSSH fluctuations and flatness of the shore. Additionally, the model was equipped with a flooding/drying algorithm, enabling the model to describe the variability of shoreline due to mean sea level change and wind surges. A more detailed description of the model used in this work is presented in (Ibrayev and Dyakonov, 2016; Dyakonov and Ibrayev, 2016).

The model configuration is described in (Dyakonov and Ibrayev, 2018), we will note only the main points here. We use the Caspian Sea bathymetry based on the ETOPO1 dataset (Amante and Eakins, 2009), particular attention has been paid to correctly interpolate the data onto the model grid and to preserve their details, such as islands and the shoreline. The Karabogaz-Gol Bay was erased from the relief, as its connection to the sea is unilateral, and the corresponding boundary condition

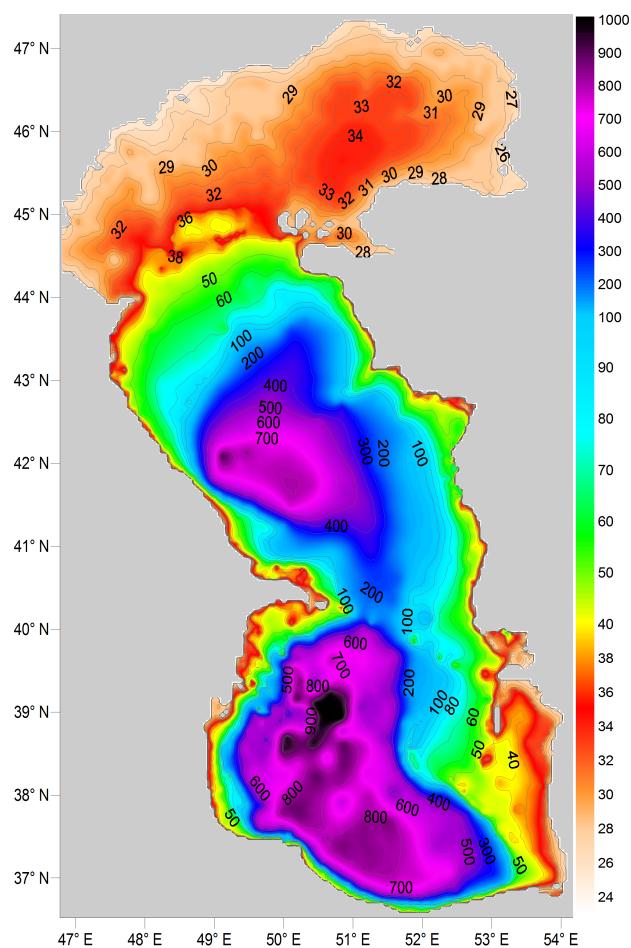


Figure 1. Caspian Sea bathymetry, used in the model (depths relative MSL, m). The average sea surface depth and model vertical grid origin are 28 m.

was set, to account for the outflow of sea water into the bay. The resulting bathymetry is presented on fig. 1. The model has a resolution ~ 4.3 km in the horizontal plane, which is relatively high, as the Rossby baroclinic deformation radius is 17–22 km in deep-water areas of the Caspian (Arkhipkin et al., 1992). Eddy-resolving ability of the model is important to adequately simulate heat and salt transfer in the sea interior and obtain a correct circulation pattern. In the vertical a rather fine grid is set:
5 from 2 m in the upper sea layer to 30 m in deep waters. This minimizes the numerical errors in the advection term discretization and prevents their excessive accumulation in the long-term. The model time step is 5 min.

2.2 External forcing

Monthly mean river runoff data were used to prescribe the discharge of the Volga, Ural, Kura, Terek and Sulak Rivers. The outflow into the Kara-Bogaz-Gol Bay was set using annual mean data. Air forcing was prescribed using the ECMWF Era-40



atmospheric reanalysis dataset (Kallberg et al., 2004), which was chosen for several reasons. First, the data cover an extended period (from 1957 to 2002), which comprises one of the most vivid episodes of the global climate change – the climatic regime shift of 1976-1978. This allows to investigate the Caspian Sea response to such global events. The other advantage of the Era-40 reanalysis is its relatively high spatial resolution (1.125°), which is still rather coarse for the Caspian Sea with dimensions $8^\circ \times 11^\circ$, but is sufficient to resolve main features of the atmospheric circulation in the region, as has been shown in (Ibrayev et al., 2010). The Era-40 temporal resolution of 6 hours allows to simulate the diurnal air-sea interaction cycle and the synoptic variability mode. As any global reanalysis product, Era-40 has errors, specific for a particular region of the planet (Berg et al., 2012; Cattiaux et al., 2013). Therefore, we have partially corrected the Era-40 wind, precipitation and solar radiation fields, based on the available climatology atlases of the Caspian region (Panin, 1987; Terziev et al., 1992). The performed corrections as well as the model sensitivity to them are considered in detail in (Dyakonov and Ibrayev, 2018). The prescribed atmospheric parameters together with the parameters of the sea surface, obtained in the model, are used to compute the air-sea fluxes: evaporation, sensible and latent heat fluxes and the momentum flux. Precipitation and radiative heat fluxes are taken directly from Era-40. The fluxes are dynamically amended due to sea ice cover, simulated in the submodel of sea ice thermodynamics, described in (Schrum and Backhaus, 1999).

2.3 Initial conditions and model “spin-up”

The model was initialized with the climatic mean 3D-fields of temperature and salinity for January (Kosarev and Tuzhilkin, 1995). These fields have been considerably smoothed and averaged over an extended period of time, and, therefore, lack realistic cross-shore gradients and many other details, particularly in shallow regions. While the distribution of temperature in such areas adjusts rather quickly due to atmospheric impact, the salinity field is a lot more inert and requires an additional “spin-up” model run: the model is run for 5 years with a relaxation of sea surface salinity (SSS) in the Southern Caspian basin. This is necessary to avoid excessive growth of salinity in the upper layer of the basin, until a fresh-water anomaly, associated mainly with the Volga River’s runoff, appears along the western coast of the Mid Caspian. It is this anomaly that supplies relatively fresh water to the south in an amount, sufficient to compensate intense evaporation. After 5 years a realistic salinity distribution in the Mid Caspian is achieved, and the SSS relaxation in the Southern Caspian is no longer required to balance the salt budget of this basin. The resultant salinity field is then used as the initial condition for the main model run, discussed further.

3 External forcing variability

Figure 2 shows the evolution of external forcing components for the period considered. The Caspian Sea water budget is a sum of river discharge ($\sim 300 \text{ km}^3 \text{ year}^{-1}$) and precipitation ($\sim 100 \text{ km}^3 \text{ year}^{-1}$) deducted by evaporation ($\sim 400 \text{ km}^3 \text{ year}^{-1}$) and the outflow into the Kara-Bogaz-Gol Bay ($\sim 30 \text{ km}^3 \text{ year}^{-1}$) (Terziev et al., 1992). The underground water contribution is thought to be insignificant ($\sim 4 \text{ km}^3 \text{ year}^{-1}$) (Zektser et al., 1984). Evaporation is the only component that cannot be directly measured, and therefore it is computed by the model based on air and sea surface parameters. The evolution of the net input of

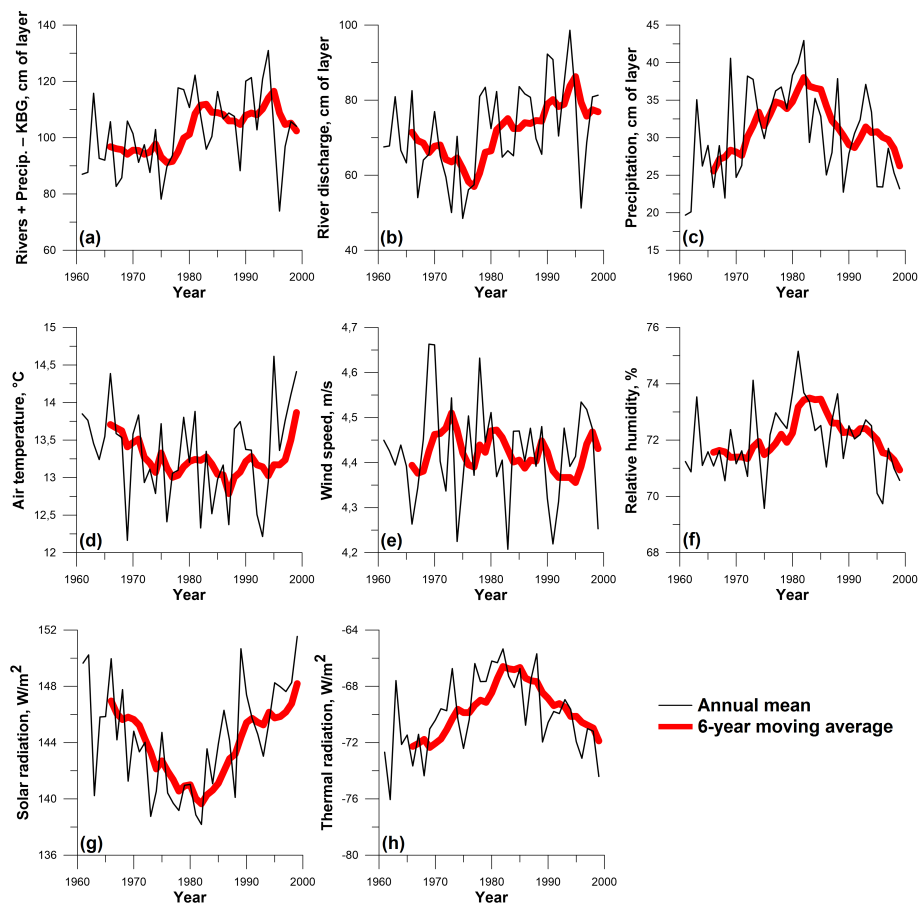


Figure 2. Long-term variability of the forcing components: (a) – sum of riverine water input and precipitation with the deduction of the outward flux into the Kara-Bogaz-Gol Bay; (b) – riverine water input alone; (c) – precipitation; (d) – air temperature ($^{\circ}\text{C}$); (e) – wind speed module (m s^{-1}); (f) – relative humidity (%); (g) – surface solar radiation (W m^{-2}); (h) – surface thermal radiation (W m^{-2}). All atmospheric parameters and fluxes were averaged over the sea area; water fluxes (a, b, c) are given in terms of the corresponding sea level increment.

the other three water budget components as well as river discharge and precipitation separately is presented on fig. 2a, 2b and 2c respectively. In the late 1970's one can note a sharp rise ($\sim 20\%$) in the net water input, which was a consequence of the climatic regime shift, mentioned earlier. The shift was also associated with an increase of air humidity in the Caspian region, followed by a trend change in the evolution of radiative fluxes: both solar and thermal radiation (absolute value) intensities began to grow after 1980. We will refrain from discussing the reasons and mechanisms of such abrupt variations and merely ascertain the fact, that the data, used to prescribe the external forcing in the model, contain the signal, associated with the climatic shift of 1976-1978. Notably, there is no significant long-term change in the average air temperature and wind speed module present in the data (fig. 2d and 2e).



4 Model reconstruction: long-term trends and circulation analysis

In this section we analyze the long-term evolution of the sea water parameters obtained in the numerical reconstruction. The Caspian Sea comprises three basins, partly separated by peninsulas extending into the sea interior: northern, central and southern (further NorthCS, MidCS and SouthCS respectively). Due to extremely different bottom relief, non-uniform distribution of river run-off and a large sea extent in the latitude direction, the thermohaline circulation patterns in each basin are very distinctive. Therefore, the analyzed properties of the water masses have been averaged over a certain horizon for every Caspian basin separately. Averaging in the horizontal plane simplifies the analysis but conceals many subbasin-scale features of the fields considered, which must be kept in mind further. On the contrary, the sea level evolution is examined in a particular point to better indicate any deviations from the measurements. On all of the following figures vertical dashed lines indicate the moments of climatic shifts.

4.1 Sea level

Figure 3 compares the observed sea level variability in the vicinity of Baku (Apsheeron Peninsula) with that obtained by the model. Until the sharp decline of 1975 there is a good match of the two curves, which indicates a correct description of the sea water balance components. Yet sharp changes of the sea level are not well reproduced due to errors in the model and/or the external forcing data, which led to a considerable discrepancy (up to 35 cm). As a result, the sea surface area is overestimated by the model, and, in turn, so is the net evaporation flux, which is why the model CSSH has a slow downtrend relative observations and matches them again in 1992. This negative feedback between the sea level and its surface area was shown to be significant in (Dyakonov and Ibrayev, 2018). We have also demonstrated in this paper, that the sea water balance is reproduced quite accurately, if the model is started from 1978 with the correct initial CSSH, which suggests, that considerable errors in the water budget components occur only in the mid-1970's. Overall, the evolution of the Caspian Sea surface height is reconstructed reasonably well, and this fact alone refutes all of the hypotheses relating its rapid rise in 1978-1995 with changes of the seabed, underground infiltration of the Aral Sea waters into the Caspian, variations of the underground water discharge and other factors that are not taken into account in the model. Indeed, our results are consistent with the theory on the dominant role of the global climate fluctuations in the Caspian Sea level variability on a decadal timescale (Frolov, 2003; Panin and Diansky et al., 2014). Thus, the sharp level growth was caused by the above mentioned climate regime shift of 1976-1978, and the corresponding signal is present in the forcing data we use (fig. 2b, 2f).

4.2 Northern Caspian

The Northern Caspian is a very shallow estuary of the Volga and Ural rivers, the circulation of its waters is strongly influenced by their discharge and wind forcing. Due to small depths (4-5 m in most of its area) the water column is almost mixed throughout the year, therefore we analyze surface properties only. Figure 4 shows the evolution of the sea surface salinity (SSS) in all of the three basins. The amplitude of the SSS annual oscillations increases northward, which is a direct consequence of the riverine run-off distribution in space. As one can see from the fig. 4, the SSS in the NorthCS basin fluctuates around 8 psu

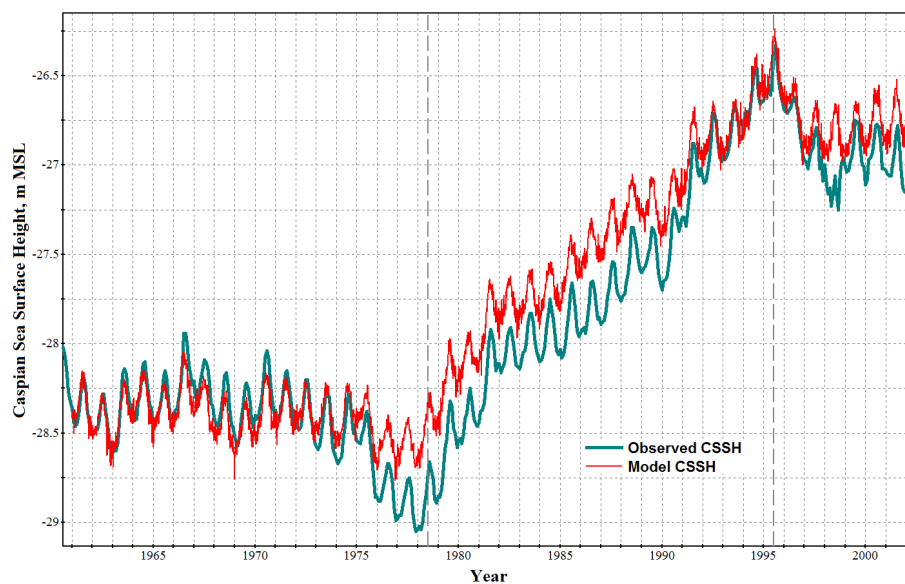


Figure 3. Caspian Sea surface height (CSSH) in the vicinity of Baku: observations and model reconstruction (m, MSL).

until the climate regime shift of 1976-1978, and then reaches a new quasi-equilibrium state with the annual mean value slightly below 7 psu. The time required for this transition period is rather small and amounts to 3-4 years. After 1980 the SSS trend stabilizes, but an additional drop down to 6 psu occurs in the 1990's. In the other two Caspian basins SSS trends are similar, but their rates are smaller by an order of magnitude. Overall, the SSS evolution in the entire sea correlates with river discharge and air humidity, and the results presented here are consistent with the observations (Tuzhilkin et al., 2011).

Noteworthy, the reconstructed evolution of the NorthCS salinity field is rather sensitive to the model design, particularly to the bottom drag parameterization. An important feature of this basin is that it serves as a transit zone for fresh riverine waters, moving into the MidCS and SouthCS basins to be evaporated there. This leads to a continuous loss of the net mass of salt in the northern basin, which can be compensated only by recurrent intrusions of the MidCS saline waters induced by wind, as shown in fig. 5b. However, such intrusions are usually brief, so the amount of salt, that enters and remains in the northern basin, greatly depends on the bottom drag resistance to the currents transporting it. The use of a too viscous bottom drag parameterization in our prior experiments caused a gradual decline of the mean NorthCS salinity down to zero within a decade. Therefore, a new parameterization scheme, that is more adequate for such shallow regions, has been devised, which allowed to stabilize the salinity evolution here at a level close to that observed. Nonetheless, the distribution of salt in NorthCS is still somewhat incorrect as compared to observations: the fresh-water tongue, associated with the Volga River, extends southward too far, often shifting salinity gradient maximum close to MidCS waters (see fig. 5a). In these conditions wind drives very fresh water masses into the MidCS basin, decreasing its surface salinity down to ~12 psu on the average (fig. 4), which is about 0.5-0.7 psu lower, than observed.

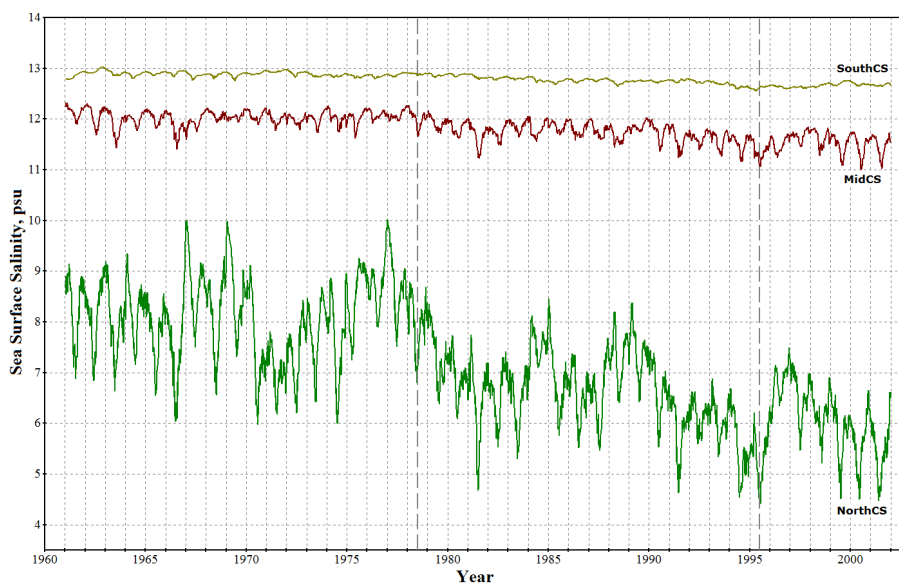


Figure 4. Evolution of the sea surface salinity (SSS), averaged over the three Caspian basins (psu).

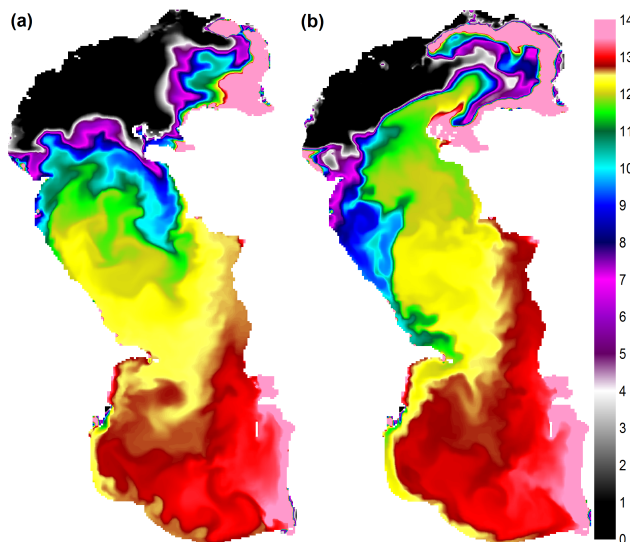


Figure 5. Sea surface salinity (psu) at two different time moments: (a) – August 1, 1974, characterized by a fresh water intrusion into MidCS from NorthCS, and (b) – July 1, 1975, reverse situation with salty MidCS waters entering NorthCS.

4.3 Mid Caspian

The Mid and Southern Caspian basins have maximum depths of 800 m and 1000 m respectively, so vertical mixing processes play a much greater role in thermohaline circulation here than in the north. In MidCS autumn-winter convection is thought



to create a mixed layer of depth 200 m and to mix the entire water column during the coldest winters, e.g. in the winter of 1969 (Terziev et al., 1992). However, the more recent papers (Tuzhilkin and Goncharov, 2008; Tuzhilkin et al., 2011) suggest, that throughout the period considered, convective mixing occurred only in the upper 100 m layer and did not reach the Caspian abyssal waters even in the most severe winters. Our results support these conclusions: in the numerical experiment the average depth of winter convection in the deep parts of the MidCS basin is about 80 m. The above mentioned 0.5-0.7 psu underestimation of MidCS surface salinity significantly decreases the convection intensity, but auxiliary sensitivity experiments have shown, that convection depth does not exceed 110-120 m, even if this error in the SSS field is artificially compensated.

Figures 6, 7, 8 show the reconstructed evolution of salinity, temperature and density at different depths in the MidCS basin. At a depth of 250 m the effects of convective mixing are noted only in the coldest winters and are absent at 500 m and below (fig. 7). In the active layer (upper 100-150 m) thermohaline properties exhibit a clear seasonal cycle and have no long-term trend until 1978, which indicates a quasi-stationary circulation regime. After the climate shift of 1976-1978 the upper layer salinities begin a gradual decline (fig. 6), associated with the intensification of river discharge and the increase of air humidity in the Caspian region. These downtrends cease only after the next climatic shift in the mid-1990's, when a new quasi-stationary sea circulation regime is achieved. Because the freshening signal, associated with the first shift, originates at the surface, the rate of the salinity downtrends decreases with depth, which strengthens sea stratification and diminishes convection-driven ventilation of deep waters. These results are in good agreement with the observations (Tuzhilkin and Kosarev, 2004; Tuzhilkin et al., 2011). The weakening of convection also accounts for the reduction of winter SST, noted after the shift of 1976-1978 in MidCS, and for the upward trend in the subsurface temperatures (fig. 7), as was suggested in (Tuzhilkin et al., 2011).

At greater depths (500 m and deeper) the influence of changes in the external conditions becomes almost indistinguishable from the accumulating model errors, that account for a slow downtrend (~ 0.1 psu / 40 years) in the average salinity and an uptrend ($\sim 1^\circ$ C / 40 years) in the average temperature. These trends are caused by advective and diffusive mixing and are inevitable in the presence on small but non-zero T and S vertical gradients. According to (Tuzhilkin and Goncharov, 2008), the only process that can counteract it, is the downsloping cascading – slow sinking of cold saline waters along the slope of the northern and eastern shelves. Despite its important role, this process is not fully taken into account by the model, which is why it yields these erroneous slow trends. In the active layer, on the contrary, the model errors do not conceal the actual variability of water properties, as the long-term trends alternate with quasi-stationary circulation regimes in correlation with the external forcing variations.

4.4 Southern Caspian

The reconstructed evolution of salinity, temperature and density in the SouthCS basin is presented in figures 9, 10, 11. The Southern Caspian basin is the most distant one from the Volga River's mouth and has the strongest evaporation throughout most of the year (Panin, 1987), therefore the salinity field in its active layer is rather sensitive to water exchange with relatively less salty MidCS basin. In order to attain a circulation regime, that would balance the salt budget of SouthCS, a 5-year spin-up model run with SSS relaxation was necessary, as we have described in section 2.3. However, after the SSS field had been released, it took three more model years to reach a quasi-equilibrium circulation in the upper 100 m sea layer (fig. 9, 10).

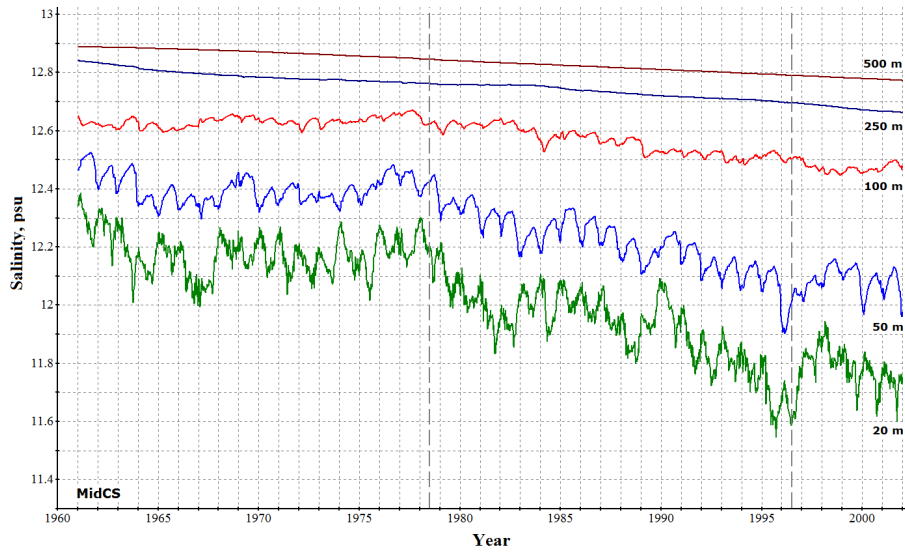


Figure 6. Evolution of the sea salinity (psu) at different depths, averaged over the MidCS basin.

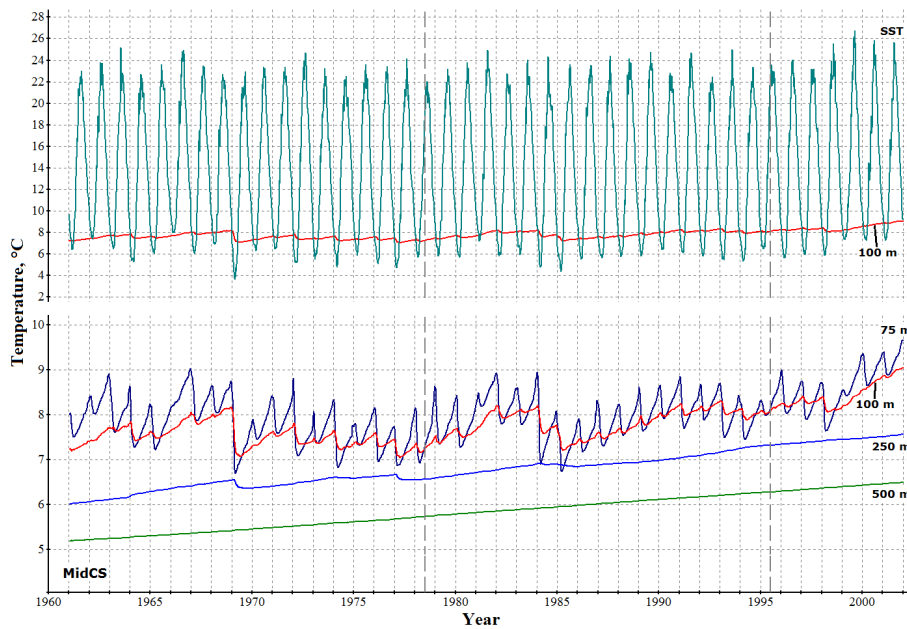


Figure 7. Evolution of the sea temperature at different depths (SST – sea surface temperature), averaged over the MidCS basin (°C).

During the first two years surface salinity grows rapidly, which leads to an intensification of convection-driven mixing in the active layer during the third year of the run with relatively sharp rises of temperature and salinity at the depth of 100 m. By the fourth year of the run (in 1964) a vertically quasi-homogeneous salinity distribution is achieved (fig. 9), characterized by a

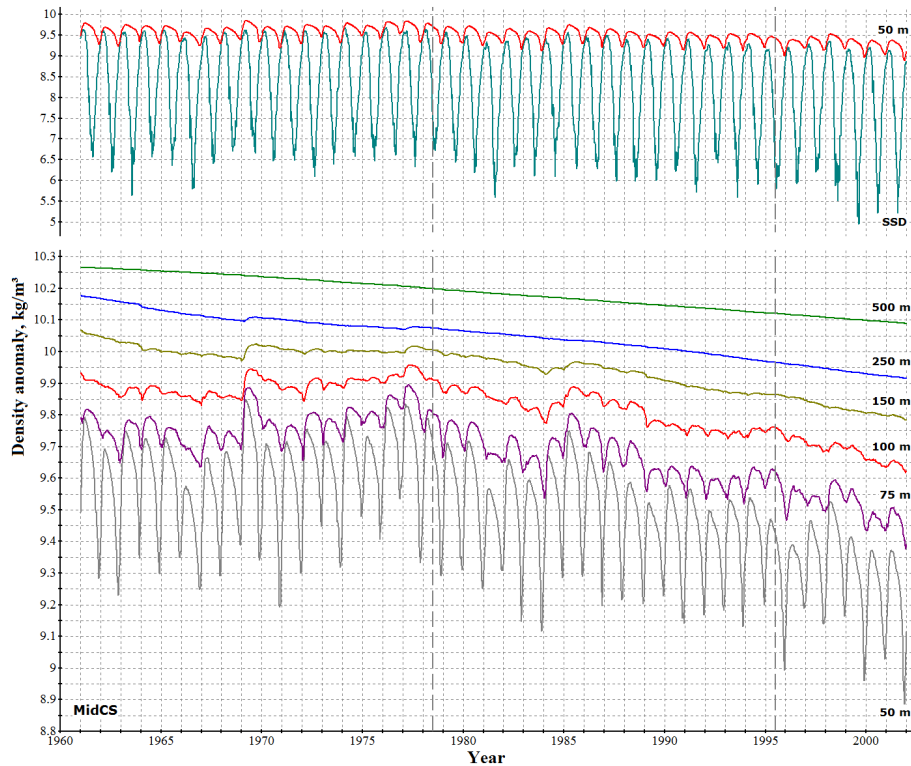


Figure 8. Evolution of the sea density anomaly (kg m^{-3}) at different depths (SSD – sea surface density), averaged over the MidCS basin.

slight positive deviation (~ 0.1 psu) in the active layer from the mean climatic data (Kosarev and Tuzhilkin, 1995). As a result, the maximum convection depth exceeds that observed by 10–15 m: in SouthCS convective mixing processes span the upper 70–80 m layer and reach 100 m only in its northern part (Terziev et al., 1992). In the model reconstruction the lower boundary of the convective mixed layer is located at the depth of 80–90 m in the central area of the basin. Thus the average temperatures at 100–150 m are overestimated by 1–2° C due to overly intense mixing with warmer surface waters during winter.

After the first four years of the model run a steady circulation regime is achieved in the upper 100 m layer, which persists until the 1980's. The impact of the climatic shift of 1976–1978 on the thermohaline properties in SouthCS is similar to that obtained in MidCS, but has a 3-year time lag, required to adjust the MidCS circulation to the forcing variation. In 1981 a transition begins to a new circulation regime, characterized by a restoration of stable salinity stratification and an additional increase of temperatures in the lower part of the active layer. Thereby autumn-winter convection in SouthCS weakens, as can be clearly seen in the evolution of density at 75 m in fig. 11. Like in the Mid Caspian, slow trends in temperature and salinity below 250–300 m in SouthCS are a result of vertical advective and diffusive mixing in absence of sufficient deep water ventilation via downsloping cascading from the eastern shelf. At the depth of 250 m the effects of the second climatic shift are still observed, and this is the maximum depth, to which a signal of external forcing variability propagates, both in MidCS and SouthCS basins.

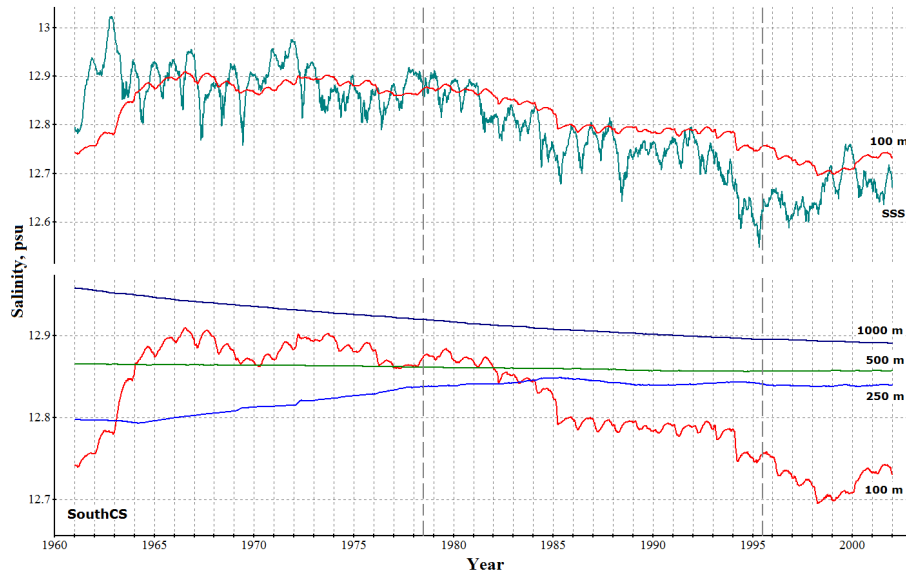


Figure 9. Evolution of the sea salinity (psu) at different depths, averaged over the SouthCS basin.

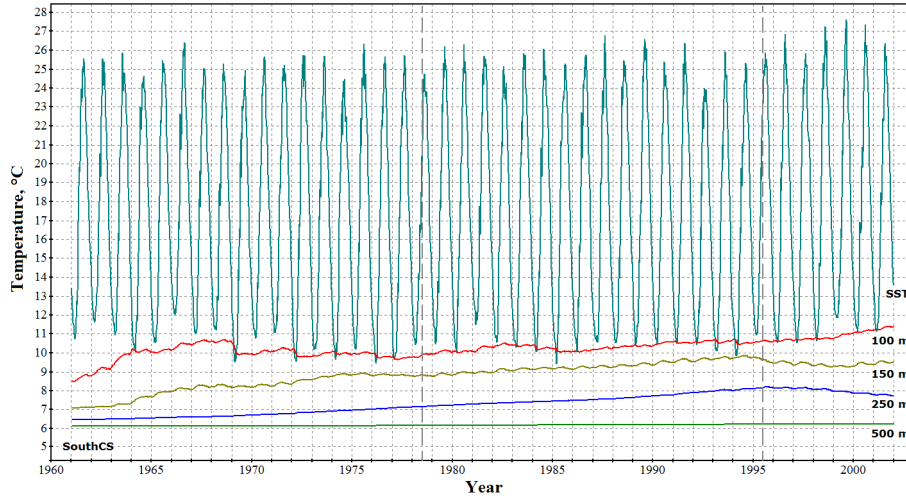


Figure 10. Evolution of the sea temperature at different depths (SST – sea surface temperature), averaged over the SouthCS basin (°C).

5 Conclusions

When modeling the Caspian Sea circulation, the greatest challenge is to keep the salinity distribution in the active layer close to that observed. Even slight errors in the salinity field significantly modulate the intensity and the depth of convective mixing and, consequently, alter the thermohaline circulation patterns of the entire sea. Two major factors determine the deviations of salinity: external forcing errors and model quality, particularly the description of the inter-basin water mass exchange, as the

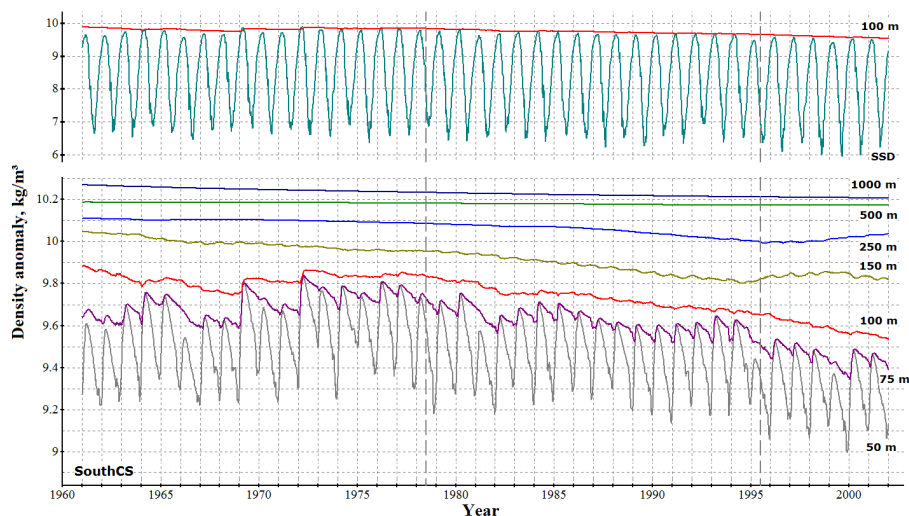


Figure 11. Evolution of the sea density anomaly (kg m^{-3}) at different depths (SSD – sea surface density), averaged over the SouthCS basin.

three Caspian basins have different salinity regimes. Correct simulation of deep water properties requires taking into account downsloping cascading, which is an important mechanism of ventilation and renewal of the abyssal Caspian waters.

Despite all of its errors and simplifications, the model qualitatively reproduced the evolution of the Caspian Sea thermohaline circulation: major features of the variability of surface level and thermohaline properties are consistent with observational data. A correct reconstruction of the water balance in 1978-1995, i.e. during the period of a rapid sea level rise (~ 2.5 m), confirms, that the level rise was associated with the variability of riverine and atmospheric forcing, rather than any factors, unaccounted for by the model. Thus, our results are consistent with the commonly recognized theory, relating the Caspian Sea level fluctuations with global climate changes.

During the first 15-17 years of the experiment a quasi-stationary circulation pattern was obtained with a clear seasonal cycle and almost no long-term trends in the evolution of temperature and salinity in the active sea layer. The depth of winter convection in the Mid Caspian, obtained in the model, is about half of that estimated in (Terziev et al., 1992), but it is in good agreement with the results of more recent studies (Tuzhilkin and Goncharov, 2008; Tuzhilkin et al., 2011). At greater depths, below the active layer, slow trends in the evolution of thermohaline properties were obtained as a result of insufficient ventilation of these waters, as the model does not fully take into account downsloping cascading processes. The error accumulation rate amounts to $\sim 1^\circ \text{C} / 40$ years for temperature and ~ 0.1 psu / 40 years for salinity. At the intermediate depths (200-300 m) both these trends and the effects of external forcing variability are noted, while below 250-300 m the latter are absent.

After 1978 the non-trend circulation mode was replaced by a transition to a new circulation regime due to a shift, that had occurred in the global climate. This transition was associated with downtrends in salinity field, which led to strengthening of density stratification in the upper sea layers and weakening of autumn-winter convection. As a result of an increased isolation from the surface waters during winter, the temperature at 100-200 m showed an uptrend. The surface salinity in the Northern



and Mid Caspian responded to the increased river discharge almost simultaneously, while the corresponding trend in the Southern Caspian SSS occurred with a 3-year time lag, which indicates a much stronger interdependence of the Mid Caspian with the northern basin rather than the southern one. Overall, the reproduced sea response to the climatic shift of 1976-1978 is consistent with the observational data analysis, presented in (Tuzhilkin et al., 2011). The next climatic shift of 1995 stabilized the salinity trends, and a new circulation regime was achieved.

Author contributions. The research was carried out by GD under the supervision of RI.

Competing interests. The authors declare that they have no conflict of interest.

Acknowledgements. The work was carried out at the Northern Water Problems Institute of the Karelian Research Center with the financial support of Russian Science Foundation grant no. 14-17-00740 “Lakes of Russia: Diagnosis and Prediction of State of Ecosystem under Climate Changes and Anthropogenic Impacts.” The research was carried out using the equipment of the shared research facilities of HPC computing resources at Lomonosov Moscow State University (Sadovnichy et al., 2013) and Joint Supercomputer Center of the Russian Academy of Sciences.



References

- Amante, C. and Eakins, B.W.: ETOPO1 1 Arc-Minute Global Relief Model: Procedures, Data Sources and Analysis, NOAA Technical Memorandum NESDIS, NGDC-24, National Geophysical Data Center, NOAA, 25 p., DOI: 10.7289/V5C8276M, 2009.
- Arkipkin, V. S., Bondarenko, A. L., Vedev, D. L. and Kosarev, A. N.: Peculiarities of water circulation at eastern coast of the Middle Caspian Sea, *Vodnye Resursy*, 6, 36-43, 1992 (in Russian).
- Arpe, K., Bengtsson, L., Golitsyn, G. S., Mokhov, I. I., Semenov, V. A. and Sporyshev, P. V.: Analysis and modeling of the hydrological regime variations in the Caspian Sea basin, *Doklady Earth Science*, 366 (4), 552–556, ISSN 1028-334X (print), 1531-8354 (electronic version), 1999.
- Berg, P., Feldmann, H. and Panitz, H.J.: Bias correction of high resolution regional climate model data, *Journal of Hydrology*, 448–449, 80–92, DOI: 10.1016/j.jhydrol.2012.04.026, 2012.
- Cattiaux, J., Douville, H. and Peings Y.: European temperatures in CMIP5: origins of present-day biases and future uncertainties, *Climate Dynamics*, 41(I), 11–12, 2889–2907, DOI: 10.1007/s00382-013-1731-y, 2013.
- Diansky, N.A., Fomin, V.V., Vyruchalkina, T.Yu., and Gusev, A.V.: Reproduction of the Caspian Sea circulation with calculation of the atmospheric forcing using the WRF model, *Trudy KarNC*, 5, 21-34 (in Russian), DOI: 10.17076/lim310, 2016.
- Dyakonov, G.S. and Ibrayev, R.A.: Description of coastline variations in an ocean general circulation model, *Izv., Atmos. Ocean. Phys.* 52, 535–541, DOI: 10.1134/S0001433816050054, 2016.
- Dyakonov, G.S. and Ibrayev, R.A.: Reproduction of interannual variability of the Caspian Sea level in a high-resolution hydrodynamic model, *Oceanology*, 58(1), 8–18, DOI: 10.1134/S0001437018010046, 2018.
- Frolov, A. V.: Modeling of the Long-Term Level Fluctuations of the Caspian Sea: Theory and Use, GEOS, Moscow, ISBN 5-89118-298-X, 2003 (in Russian).
- Gunduz, M. and Özsoy, E.: Modeling seasonal circulation and thermohaline structure of the Caspian Sea, *Ocean Sci.*, 10, 459–471, DOI:10.5194/os-10-459-2014, 2014.
- Ibrayev, R. A.: Model of enclosed and semi-enclosed sea hydrodynamics, *Russ. J. Numer. Anal. M.*, 16(4), 291–304, DOI: 10.1515/rnam-2001-0404, 2001.
- Ibrayev, R. A.: Mathematical Modeling of Thermodynamics Processes in the Caspian Sea, GEOS, Moscow, ISBN 978-5-89118-418-3, 2008 (in Russian).
- Ibrayev, R.A. and Dyakonov, G.S.: Modeling of ocean dynamics with large variations in sea level, *Izv. Atmos. Ocean. Phys.*, 52, 455–466, DOI: 10.1134/S000143381604006X, 2016.
- Ibrayev R. A., Ozsoy E., Schrum C. and Sur H. I.: Seasonal variability of the Caspian Sea three-dimensional circulation, sea level and air-sea interaction, *Ocean Sci.*, 6, 311–329, DOI: 10.5194/os-6-311-2010, 2010.
- Ibrayev, R. A., Sarkisyan, A. S., and Trukhchev, D. I.: Seasonal variability of the circulation of the Caspian Sea reconstructed from mean multi-year hydrological data, *Izvestiya, Atmos. Ocean. Phys.*, 37(1), 96–104, 2001.
- Kallberg, P., Simmons, A., Uppala, S. and M. Fuentes: ERA-40 Project Report Series No. 17, European Centre for Medium Range Weather Forecasts, Reading, 2004.
- Kara, A. B., Wallcraft, A. J., Metzger, E. J. and Gunduz, M.: Impacts of freshwater on the seasonal variations of surface salinity and circulation in the Caspian Sea, *Cont. Shelf Res.* 30 10–11, 1211–1225, DOI: 10.1016/j.csr.2010.03.011, 2010.



- Kosarev, A. N. and Tuzhilkin, V. S.: Climatic Thermohaline Fields in the Caspian Sea, Sorbis, Moscow, 92 p., ISBN 5-88403-004-6, 1995 (in Russian).
- Miller, A.J., Cayan, D.R., Barnett, T.P., Graham, N.E. and Oberhuber, J.M.: The 1976-77 climate shift of the Pacific Ocean, *Oceanography*, 7(1), 21–26, 1994.
- 5 Panin, G. N.: Evaporation and Heat Exchange in the Caspian Sea, Nauka, Moscow, 88 p., 1987 (in Russian).
- Panin, G. N. and Diansky, N. A.: On the correlation between oscillations of the Caspian Sea level and the North Atlantic climate, *Izv. Atmos. Ocean. Phys.*, 50, 266–277, DOI: 10.7868/S0002351514020084, 2014.
- Powell, A. M. Jr. and Xu, J.: Abrupt Climate Regime Shifts, Their Potential Forcing and Fisheries Impacts, *Atmospheric and Climate Sciences*, 1, 33-47, DOI: 10.4236/acs.2011.12004, 2011.
- 10 Sadovnichy, V., Tikhonravov, A., Voevodin, VI. and Opanasenko, V.: "Lomonosov": Supercomputing at Moscow State University. In Contemporary High Performance Computing: From Petascale toward Exascale, Chapman & Hall/CRC Computational Science, pp. 283-307, Boca Raton, USA, CRC Press, ISBN: 9781466568358, 2013.
- Schrum, C. and Backhaus, J. O.: Sensitivity of atmosphere-ocean heat exchange and heat content in North Sea and Baltic Sea: a comparative assessment, *Tellus A*, 51, 526–549, DOI: 10.1034/j.1600-0870.1992.00006.x, 1999.
- 15 Terziev, F. S., Kosarev, A. N. and Kerimov, A. A. (ed.): Hydrometeorology and Hydrochemistry of the Soviet Seas, Vol. 6: The Caspian Sea, No. 1: Hydrometeorological Conditions, Gidrometeoizdat, St. Petersburg, 1992 (in Russian).
- Tuzhilkin, V.S. and Goncharov, A.V.: On deep water ventilation in the Caspian Sea, *Trudy GOIN*, 211, 43-64, ISSN: 0371-7119, 2008 (in Russian).
- Tuzhilkin, B.S. and Kosarev, A.N.: Long-term variations in the vertical thermohaline structure in deep-water zones of the Caspian Sea, *Water Resources*, 31 (4), 376-383, DOI: 10.1023/B:WARE.0000035677.81204.07, 2004.
- 20 Tuzhilkin, V.S., Kosarev, A.N., Arkhipkin, V.S. and Nikonova, R.E.: Long-term variations of the hydrological regime of the Caspian Sea, *Vestnik Moskovskogo Universiteta Geography*, 2, 62–71, 2011 (in Russian).
- Wooster, W.S. and Zhang, C. I.: Regime shifts in the North Pacific: early indications of the 1976-1977 event, *Progress in Oceanography*, 60, 183-200, DOI: 10.1016/j.pocean.2004.02.005, 2004.
- 25 Zektser, I. S., Dzhamalov, R. G. and Meskheteli, A. V.: Underground Water Balance between Land and Sea, Gidrometeoizdat, Leningrad, 206 p., 1984 (in Russian).